



Attorney Docket No. 8793-52026

PATENT

IN THE UNITED STATES PATENT AND TRADEMARK OFFICE

Re Application Of: Bellaiche, L., et al.

Appl. No.: 10/632,740

Group Art Unit: 1755

Filed: 08/01/2003

Examiner: Koslow, C.

For: Enhanced Electromechanical Properties in Atomically-Ordered Ferroelectric Alloys

**Mail Stop RCE
Commissioner for Patents
P.O. Box 1450
Alexandria, VA 22313-1450**

DECLARATION UNDER 37 CFR 1.132

Laurent Bellaiche declares as follows:

1. I am one of the joint inventors of the invention described and claimed in the referenced patent application.
2. Mohammed, M. et al., Temperature dependence of conventional and effective pyroelectric coefficients for compositionally graded $\text{Ba}_x\text{Sr}_{1-x}\text{TiO}_3$ films, Journal of Applied Physics 84 (6), 3322-3325, 15 September 1998 (attached hereto as Exhibit D) discloses the preparation of ferroelectric thin films of $\text{Ba}_x\text{Sr}_{1-x}\text{TiO}_3$ with gradients in composition normal to the growth surface using metalorganic decomposition. Note Fig. 1.
3. Brazier, M. et al., Unconventional hysteresis behavior in compositionally graded $\text{Pb}(\text{Zr},\text{Ti})\text{O}_3$ thin films, Applied Physics Letters, 72 (9), 1121-1123, 2 March 1998

(attached hereto as Exhibit E) discloses the preparation of thin film lead-zirconate – titanate (PZT) capacitors with composition gradients normal to the substrate using pulsed laser deposition. Note Fig. 1.

4. Exhibits D and E show that it was known to those skilled in the art at the time the present application was filed that it is possible to grow ferroelectric systems having different layers of solid solutions with differing compositions.

5. I further declare that all statements made herein of my own knowledge are true and that all statements made on information and belief are believed to be true; and further that these statements were made with the knowledge that willful false statements and the like so made are punishable by fine or imprisonment, or both, under Section 1001 of Title 18 of the United States Code, and that such willful false statements may jeopardize the validity of the above-referenced application or any patent issuing thereon.

Date: 08/02/06



Laurent Bellaiche

Temperature dependence of conventional and effective pyroelectric coefficients for compositionally graded $\text{Ba}_x\text{Sr}_{1-x}\text{TiO}_3$ films

Majed S. Mohammed and Gregory W. Auner^{a)}

Department of Electrical and Computer Engineering, Wayne State University, Detroit, Michigan 48202

Ratna Naik

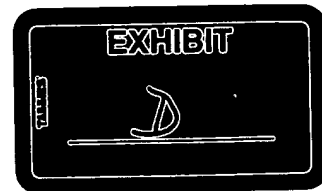
Department of Physics and Astronomy, Wayne State University, Detroit, Michigan 48202

Joseph V. Mantese, Norman W. Schubring, Adolph L. Micheli,
and Antonio B. Catalan

*General Motors Research and Development Laboratories, Electrical and Electronics Department,
30500 Mound Road, Warren, Michigan 48090-9055*

(Received 15 January 1998; accepted for publication 15 June 1998)

Ferroelectric thin films ($\sim 1.2 \mu\text{m}$) of $\text{Ba}_x\text{Sr}_{1-x}\text{TiO}_3$ with gradients in composition normal to the growth surface were formed on platinum substrates by metalorganic decomposition. Effective (pseudo) pyroelectric coefficients as large as $0.06 \mu\text{C}/\text{cm}^2 \text{K}$ have been obtained from these active ferroelectric devices under the application of an ac field (charge pumping). In contrast, a value of only $-0.003 \mu\text{C}/\text{cm}^2 \text{K}$ has been measured for the conventional pyroelectric coefficient. © 1998 American Institute of Physics. [S0021-8979(98)03118-1]



INTRODUCTION

Currently available infrared detectors can be divided into two main classes, photon and thermal detectors. In photon detectors the absorption of infrared photons causes the release of free electrons (or holes) within the sensing element. Typically a photoconductive or a photovoltaic p - n junction is made from mercury cadmium telluride (MCT) or a Si-Pt-Si Schottky barrier. In order to suppress thermal excitation of free carriers, photon detectors must be cooled to temperatures well below room temperature. The most widely used photon detector, $\text{Cd}_{0.2}\text{Hg}_{0.8}\text{Te}$ operating in the 8 – $12 \mu\text{m}$ atmospheric window, must be cooled to liquid nitrogen temperature, 77 K , for optimum performance.¹ Thermal detectors, on the other hand, usually require single stage cooling around room temperature, although they can operate adequately over a wide range of temperatures. The tradeoff, however, is that the sensitivity of thermal detectors is greatly inferior to that of photon detectors and therefore have (so far) been limited to applications that do not require extremely high sensitivity or fast response, such as surveillance, fire fighting, and low contrast thermal imaging.

The most efficient thermal detectors are made from ferroelectric materials operating as pyroelectrics.² The incident photon flux is first absorbed and converted into a temperature variation which induces a change in the dipole moment volume density (polarization) of the material. Concurrently, an induced voltage difference across the detector (operating as a capacitor) proportional to the variation in temperature will exist as a result of the change in the surface charge density.³ Ferroelectric thermal detectors are usually designed as "hybrid solder bump" structures and formed

from single crystal ferroelectrics operating either well below transition temperature (T_c) or near the transition temperature under a dc electric field bias.⁴ The former, e.g., LiTaO_3 , are characterized by low permittivity, high voltage response, and good stability, and are mainly used for large area detectors. The latter, such as potassium tantalum niobate (KTN), barium strontium titanate (BST) and La doped lead zirconate titanate (PZT), are based upon the induced pyroelectric effect near the phase transition of these materials. The transition temperature can be varied by appropriately varying the ratios of the chemical constituents. Because of this latter property, the maximum infrared response can be adjusted over a wide range of operating ambient temperatures. For example, maximum room temperature infrared response for BST single crystals occurs at a Ba/Sr ratio of 65/35, where a sharp maximum in dielectric constant, typically 30 000, is observed.⁴

A new infrared detection system based on graded ferroelectric devices (GFDs) is currently being investigated at the General Motors Research and Development Center.^{5–7} This work is motivated by the need to develop new materials that can be directly deposited in thin film form with high pyroelectric sensitivity compared to single crystal infrared detectors. Detectors made from polycrystalline ferroelectric thin films, compared to single crystal or bulk ceramic materials, are easier to fabricate and thus have the advantage of lower fabrication cost, although they currently show lower responsivity due to their lower pyroelectric coefficients.⁸

The first graded ferroelectric device was made from KTN films formed on platinum coated polycrystalline yttria by metalorganic decomposition (MOD).⁵ More recently GFDs were made from BST films formed on platinum using the same deposition technique.⁹ In these structures there is a dipole moment density gradient normal to the growth surface resulting from a gradient in composition.

^{a)}Electronic mail: gauner@ece.eng.wayne.edu

When polarization graded ferroelectric films are excited with a strong periodic electric field, a quite distinct vertical shift in the displacement (ΔD) versus field (E) hysteresis loop is observed along the displacement axis, i.e., charge pumping. The magnitude and sense of these shifts are a function of the maximum applied field, the temperature, and the polarization gradient. An effective (pseudo), pyroelectric coefficient has been defined as⁹

$$p_{\text{eff}} \equiv \frac{1}{A} \frac{d(\Delta Q)}{dT} \quad (1)$$

Here, ΔQ is the change in offset charge stored on the sampling capacitor and measured from the hysteresis loops, ΔT is the change in temperature, and A is the active device area. It has been predicted⁹ that $p_{\text{eff}} \sim E^4 (\nabla c / c_0)$, where ∇c is the composition gradient and E is the maximum applied periodic field, and $\gamma \approx 4$. As reported elsewhere,⁵ the effective pyroelectric coefficient obtained from a 9.8 μm thick graded KTN was ($\sim 10 \mu\text{C}/\text{cm}^2 \text{ K}$), many orders of magnitude greater than the conventionally measured pyroelectric coefficients obtained from the same graded KTN structure as well as that obtained from homogeneous KTN films with similar thickness. In this article we describe the steps involved in making a 1.2 μm thick graded BST film formed on platinum using MOD. A comparison between the pyroelectric coefficients obtained from rate of change of relative permittivity and polarization with temperature (or "conventional pyroelectric coefficient") and the pyroelectric coefficients measured from the shift in the hysteresis loops (or "effective pyroelectric coefficients") for these structures is given.

EXPERIMENT

Metalorganic decomposition is a simple, low-cost, non vacuum technique for making thin films.^{6,10} In our study, two multimetal carboxylate precursor solutions were prepared from barium and strontium neodecanoates (solid) and titanium IV 2-ethylhexoxide (liquid). The chemicals were combined in the proper proportions to obtain the desired stoichiometric balance. Xylene and neodecanoic acid were added to adjust the viscosity and to maintain the consistency of the metalorganic solutions. Three solutions in the proportions Ba:Sr:Ti=0.9:0.1:1, 0.8:0.2:1, and 0.7:0.3:1 were prepared by mixing together set amounts from each of the BaTiO₃ and SrTiO₃ solutions. GFD structures were formed on 1/2 in. \times 1/2 in. platinum substrates by sequentially depositing two layers of each composition onto each substrate. The BaTiO₃ layers were deposited first and the Ba_{0.7}Sr_{0.3}TiO₃ layers deposited last. The film formation process starts by dispensing the liquid metalorganic solution onto the substrate followed by its rapid rotation at a rate of 4000 rpm for 30 s. The remaining solvents in the film were removed by prebaking the sample for 2 min in air on a hot plate set at 150 °C surface temperature. Pyrolysis was carried out for 3 min in an air muffle furnace set to a temperature of 600 °C. The above process was repeated for each subsequent layer; see Fig. 1. Final anneals were carried out in flowing oxygen at

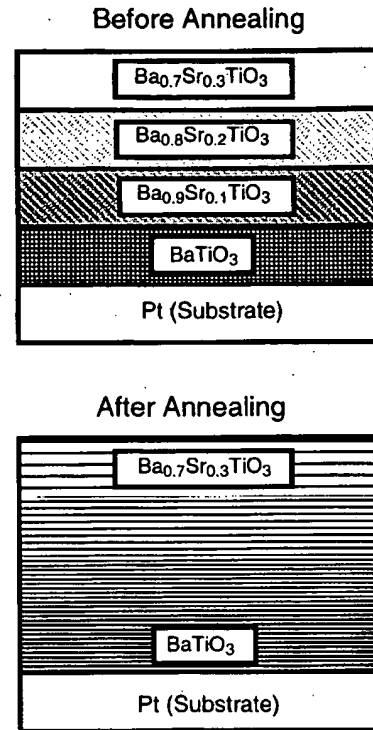


FIG. 1. Schematic of the BST GFD structure prior to and after annealing.

1000 °C for 30 min. The film thickness was measured with a Dektak 330 profilometer and found to be approximately 1.2 μm thick.

To complete the GFD structures, 0.02 cm² circular electrodes were deposited onto the film. Each electrode consisted of a 600 Å thick chromium layer (deposited first) followed by a 3000 Å thick gold layer. Small signal ac capacitance and dissipation versus temperature measurements were made under vacuum using a Hewlett-Packard 4192A LCR impedance analyzer. The temperature was regulated within ± 0.05 °C with an MMR Technologies, Inc. low temperature microprobe station. A modified Sawyer–Tower hysteresis circuit was used to measure the spontaneous polarization (P_s), remnant polarization (P_r), and the coercive field (E_c) at various frequencies and excitation levels.^{6,9} The above measurements were carried out as a function of temperature in the range of -40 to 100 °C.

RESULTS AND DISCUSSION

In the absence of internal and external strains, the macroscopic electric displacement, D , of a ferroelectric material can be written as the sum of two terms, $D = \epsilon E + P_s$. Here, ϵ is the permittivity of the material and P_s is the spontaneous polarization. Of primary interest for pyroelectric materials is the electrical response (i.e., the displacement of electric charge) of the material due to a change in temperature. For constant electric field the conventional pyroelectric coefficient is defined as

$$p = \left(\frac{\partial D}{\partial T} \right)_E = \left(\frac{\partial \epsilon}{\partial T} \right)_E E + \left(\frac{\partial P_s}{\partial T} \right)_E \quad (2)$$

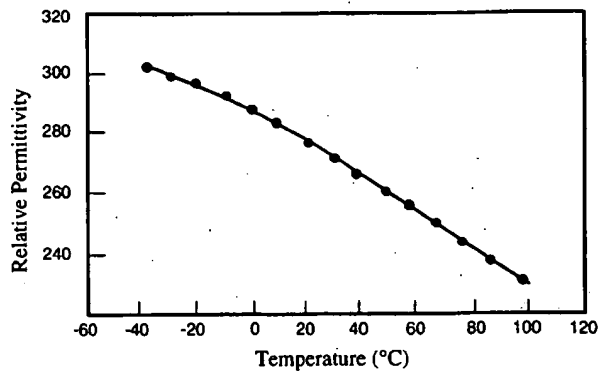


FIG. 2. Relative permittivity (ϵ/ϵ_0) of the BST GFD structure as a function of temperature.

A broad peak in the permittivity plot centered at the transition temperature is normally observed in homogeneous BST films with grain sizes on the order of $0.1\ \mu\text{m}$. In our BST GFDs the dielectric constant decreased continuously with increasing temperature as shown in Fig. 2, an expected result.⁵⁻⁷ Prior to annealing, the GFD structure can be thought of as formed from different ferroelectric layers, each with a distinct transition temperature. If these layers were to remain unaffected by the annealing process, i.e., little or no chemical diffusion occurs between layers, one would expect to see the individual peaks corresponding to each transition temperature, although highly broadened. However, a prerequisite to achieve "charge pumping" is that the change in composition or polarization in the GFD films must continuously and smoothly vary through film thickness. Thus, annealing the GFDs at relatively high temperatures ($1000\ ^\circ\text{C}$) was necessary to form the composition gradient as well as to enhance grain growth. Chemical analysis after annealing of the GFDs using x-ray photospectroscopy (XPS) depth profiling shows that the Ba/Sr ratio varies monotonically with depth through the device.

A plot of the spontaneous polarization, P_s , versus temperature, Fig. 3, shows a decrease in polarization density with increasing temperature, in contrast to the sharp drop in polarization observed in single crystal and high quality ceramic ferroelectric materials at their transition temperature. The values obtained for P_s in BST GFDs are an order of

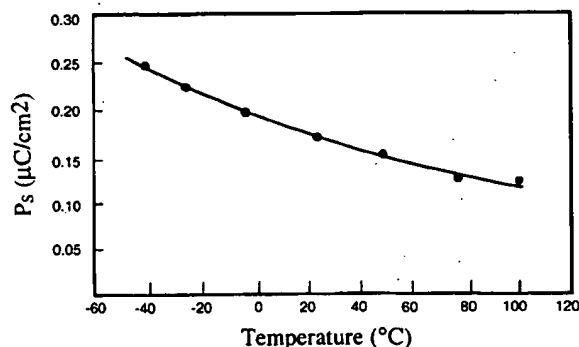


FIG. 3. Spontaneous polarization (P_s) of the BST GFD structure as a function of temperature.

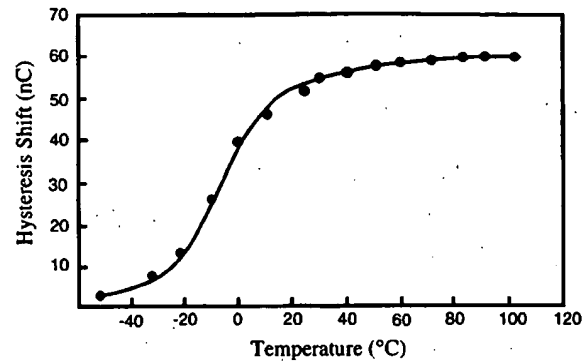


FIG. 4. Vertical shift of the D vs E hysteresis loops ($\Delta Q = \Delta D A$, with A the device area) for the BST GFD structure as a function of temperature.

magnitude less than those obtained in a previous study on homogeneous barium titanate and BST films prepared under similar conditions.⁶ As the temperature increases, the loss tangent remains more or less constant at the relatively small value of 0.015.

The change in surface charge of the BST GFDs when excited with an ac signal is $\Delta Q = C_{in} \Delta V$, where C_{in} is a $0.1\ \mu\text{F}$ sampling capacitor connected in series with the BST GFD in the Sawyer-Tower circuit, and ΔV is the vertical shift in the hysteresis loops measured in volts. Figure 4 shows the dependence of the hysteresis shifts on temperature when excited with a $1\ \text{kHz}$ @ $5\ \text{V}_{\text{peak}}/\mu\text{m}$ sinusoidal field. Between -50 and $-30\ ^\circ\text{C}$, the charge generated at the surface of the sampling capacitor slowly varies with temperature, while a sharp increase in ΔQ was observed between -30 and $25\ ^\circ\text{C}$. Finally, ΔQ was essentially constant in the interval between 25 and $100\ ^\circ\text{C}$.

Unlike homogeneous BST films, the BST GFDs in this study were formed from a range of compositions and thus did not have a single ferroelectric transition temperature, but rather an associated range of transition temperatures with upper and lower values corresponding to that of BaTiO_3 ($T_c = 130\ ^\circ\text{C}$) and $\text{Ba}_{0.7}\text{Sr}_{0.3}\text{TiO}_3$ ($T_c = 25\ ^\circ\text{C}$), respectively.

The conventional pyroelectric coefficient, as calculated from Eq. (2), with an applied field of $5\ \text{V}_{\text{peak}}/\mu\text{m}$ is shown in Fig. 5. It has a negative sign and its magnitude increases with increasing temperature. At room temperature the absolute

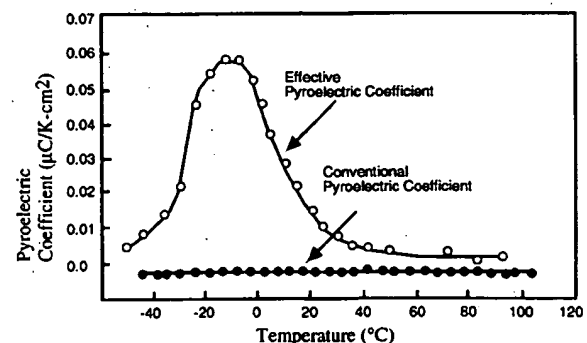


FIG. 5. Conventionally measured pyroelectric coefficient (p) and effective pyroelectric coefficient (p_{eff}), for the BST GFD structure as a function of temperature.

value of p is $0.003 \mu\text{C}/\text{cm}^2 \text{ K}$. This value is an order of magnitude smaller than that obtained for homogeneous BST 70/30 thin films⁶ ($p = 0.045 \mu\text{C}/\text{cm}^2 \text{ K}$) and several orders of magnitude smaller than that observed in homogeneous BST 65/35 single crystals and ceramics^{2,11} which have values in the range of 0.1 to $23 \mu\text{C}/\text{cm}^2 \text{ K}$.

The effective pyroelectric coefficient, defined in Eq. (1), can be easily estimated from Fig. 4. A plot of p_{eff} versus temperature is shown in Fig. 5. The effective pyroelectric coefficient has a maximum value of $0.06 \mu\text{C}/\text{cm}^2 \text{ K}$ at $T = -10^\circ\text{C}$ with an $E^{3.9}$ dependence in agreement with theoretical prediction.⁹ For BST GFDs, at low temperatures, the difference from the conventional coefficient is significant and reaches a maximum value of $p_{\text{eff}}/p=30$ at $T = -10^\circ\text{C}$. At higher temperatures the effective pyroelectric coefficient value decreases continuously and slowly approaches the value of the conventional pyroelectric coefficient.

In the present study, the advantage of using the effective pyroelectric coefficient in BST GFDs over that of the conventional effect in homogeneous BST films is clearly not significant. However, it should be mentioned here that the main objective in fabricating these films was not to optimize this effective pyroelectric coefficient but rather to demonstrate how an effective pyroelectric coefficient could be derived from the charge pumping action observed in graded BST films. The strong dependence of the pyroelectric coefficient on applied field⁹ indicates that with even a slight increase in applied voltage across the GFD film a significantly greater pyroelectric coefficient could be obtained. Increases in field were, however, not possible for these GFDs as an increase in field beyond the reported $5 V_{\text{peak}}/\mu\text{m}$ led to field breakdown.

Polycrystalline BST GFD thin film represents a significant approach in the quest to find a method of combining the

advantages of low-cost thin film processing with the high sensitivity of bulk ceramic and single crystal materials. It is clear, however, that there are several obstacles that must be overcome before these results can be utilized in a ready-for-market device. A major impediment associated with this method of forming GFDs is the high annealing temperature necessary to form the composition gradient together with the formation of only a limited step-variable polarization gradient, thus making the BST GFDs fabrication process used in this study incompatible with conventional silicon integrated circuit technology. A study is currently underway, however, to determine how such factors as film thickness, composition gradient, magnitude, and frequency of the applied voltage can be manipulated in a controlled manner to produce an optimum effective pyroelectric coefficient.

¹C. Lucas, *Sens. Actuators A* **25–27**, 147 (1991).

²R. W. Whatmore, P. C. Osbond, and N. M. Shorrocks, *Ferroelectrics* **76**, 351 (1987).

³P. W. Kruse, *Proceedings of the 9th International Symposium on Applied Ferroelectrics* (IEEE, New York, 1994), p. 643.

⁴C. Hanson and H. Beratan, in Ref. 3, p. 657.

⁵N. W. Schubring, J. V. Mantese, A. L. Micheli, A. B. Catalan, and R. J. Lopez, *Phys. Rev. Lett.* **68**, 1778 (1992).

⁶M. S. Mohammed, R. Naik, J. V. Mantese, N. W. Schubring, A. L. Micheli, and A. B. Catalan, *J. Mater. Res.* **11**, 2588 (1996).

⁷J. V. Mantese, N. W. Schubring, A. L. Micheli, and A. B. Catalan, *Appl. Phys. Lett.* **67**, 721 (1995).

⁸B. Cole, R. Horning, B. Johnson, K. Nguyen, P. W. Kruse, and M. C. Foote, in Ref. 3, p. 653.

⁹J. V. Mantese, N. W. Schubring, A. L. Micheli, M. S. Mohammed, R. Naik, and G. W. Auner, *Appl. Phys. Lett.* **71**, 2047 (1997).

¹⁰J. V. Mantese, A. L. Micheli, A. H. Hamdi, and R. W. Vest, *MRS Bull.* **XIV**, 48 (October 1989).

¹¹B. M. Kulwicki, A. Amin, H. Beratan, and C. Hanson, *Proceedings of the 8th International Symposium on Applied Ferroelectrics* (IEEE, New York (1992), p. 1.

Unconventional hysteresis behavior in compositionally graded $\text{Pb}(\text{Zr,Ti})\text{O}_3$ thin films

Mark Brazier and M. McElfresh

Department of Physics, Purdue University, West Lafayette, Indiana 47907

Said Mansour^{a)}

School of Materials Engineering, Purdue University, West Lafayette, Indiana 47907

(Received 24 November 1997; accepted for publication 31 December 1997)

Thin-film lead-zirconate-titanate (PZT) capacitors with composition gradients normal to the substrate were fabricated via a novel technique using pulsed laser deposition. These capacitors exhibited large polarization offsets when driven by an alternating electric field. The direction of the offsets depended on the direction of the gradient with respect to the substrate. The largest offset, greater than $400 \mu\text{C}/\text{cm}^2$ when driven with a $50 \text{ V}/\mu\text{m}$ field, was nearly an order of magnitude greater than any reported for other graded ferroelectric films. This difference is attributed to both the high spontaneous polarization of PZT and the high-quality films obtained by pulsed laser deposition.

© 1998 American Institute of Physics. [S0003-6951(98)01609-X]

Recently, ferroelectric films with composition gradients normal to the substrate have been reported to exhibit striking new properties^{1,2} not observed in conventional ferroelectric films. These properties have not yet been fully explored, are not well understood, and may lead to a wealth of new device applications. The most notable property of these graded ferroelectric devices, or GFDs, is the large dc polarization offset they develop when driven by an alternating electric field. Furthermore, the direction of the offset is related to the direction of the composition gradient with respect to the substrate. These offsets have been reported to have a strong temperature dependence² giving rise to possible pyroelectric applications in addition to other potential sensor, actuator, and energy converter applications.

The composition gradients found in early GFDs were not intentional. They were merely artifacts of the processing method¹ and, thus, difficult to reproduce. Quite recently, however, $(\text{Ba,Sr})\text{TiO}_3$ (BST) films fabricated with intentional composition gradients have been reported.² The gradients were achieved by depositing discrete layers of BST with varying compositions via metallo-organic deposition, a spin-on method. Formation of a smooth gradient relied on subsequent high-temperature annealing to facilitate interdiffusion of the discrete layers. These graded BST devices have exhibited polarization offsets as large as $60 \mu\text{C}/\text{cm}^2$ when driven by a $7 \text{ V}/\mu\text{m}$ alternating field. This polarization offset is an order of magnitude greater than values of spontaneous polarization typically observed in conventional BST films.³

The primary inquiry of the research reported here was whether compositionally graded $\text{Pb}(\text{Zr,Ti})\text{O}_3$ (PZT) films would exhibit similar polarization offsets when driven by an alternating electric field. A secondary hypothesis was that the greater spontaneous polarization of PZT⁴ and the fabrication of highly epitaxial films using pulsed laser deposition^{5,6} would result in larger polarization offsets than those observed in the graded BST devices. Furthermore, the forma-

tion of the composition gradient required no high-temperature anneal making it suitable for integration with silicon technology.

The composition gradient was achieved by means of a novel technique for growing compositionally varied multilayer structures using pulsed laser deposition. The deposition method employed two half-targets with compositions of $\text{PbZr}_{0.75}\text{Ti}_{0.25}\text{O}_3$, PZT (75/25), and $\text{PbZr}_{0.55}\text{Ti}_{0.45}\text{O}_3$, PZT (55/45). The half-targets were placed adjacent to one another with the interface at a 45° angle to the vertical. The laser beam was then rastered across the target horizontally while its vertical position was incrementally increased after each horizontal scan as shown in Fig. 1. For each horizontal scan a combination of discrete layers of either composition was deposited. Initially, a layer of PZT (75/25) was deposited. During the next scan a thin layer of PZT (55/45) was deposited as well as a layer of PZT (75/25). With each successive scan the layers of PZT (75/25) deposited became thinner while those of PZT (55/45) deposited became thicker, ending with a final layer of PZT (55/45). For convenience, films with Zr/Ti ratios varying from PZT (75/25) at the substrate to PZT (55/45) at the top surface will be referred to as "up" or "up-graded." Films with the opposite gradient will hereafter be referred to as "down" or "down-graded." In this manner, both up-graded and down-graded films were deposited on Pt-coated Si substrates held at 600°C in 300 mTorr of O_2 . A total of 15 horizontal scans on

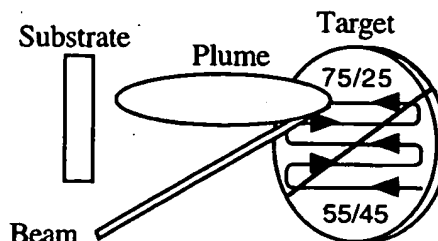


FIG. 1. Method using pulsed laser deposition to grow a compositionally graded film. Laser is raster controlled to follow the pattern on target shown.

^{a)}Electronic mail: said@ecn.purdue.edu

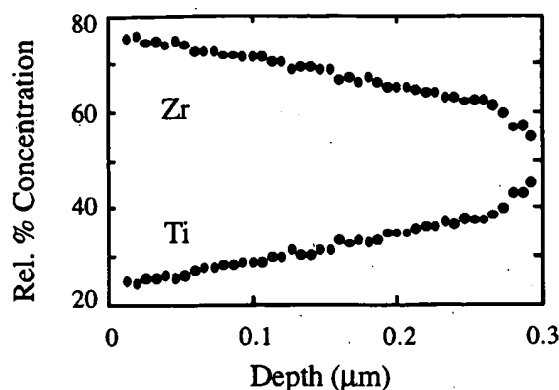


FIG. 2. Auger depth profile showing Zr and Ti content for a typical "down-graded" film.

the target were performed resulting in a film thickness of 0.3 μm . Top electrodes, an array of 50 μm by 50 μm Pt pads, were formed via photolithography and sputtering. A small section of the substrate was masked off during deposition to allow access to the bottom Pt electrode.

The relative Zr/Ti concentration of the films as a function of depth was determined using a combination of Auger electron spectroscopy and ion milling to construct a depth profile. X-ray diffraction was used to determine crystallinity and orientation of the films. Hysteresis loops (polarization versus applied field) were measured using a modified Sawyer-Tower circuit⁷ dc coupled to a digitizing oscilloscope using a 1 kHz sinusoidal driving field that varied from 0 to ± 50 V/ μm (100 V/ μm peak to peak).

The results of Auger depth profiling are shown in Fig. 2. The resulting plot is the relative concentration of Zr and Ti, as a function of depth for a typical down-graded film. The depth profile indicates that the deposition method produces smooth, linear composition gradients, either from PZT (75/25) to PZT (55/45), or vice versa. X-ray diffraction measurements were also consistent with the presence of a range of compositions in the films rather than discrete layers of PZT (55/45) and PZT (75/25). The (200) peak of the up-film is shown in Fig. 3 along with the (200) peaks for conventional 55/45 and 75/25 films. It is known that the

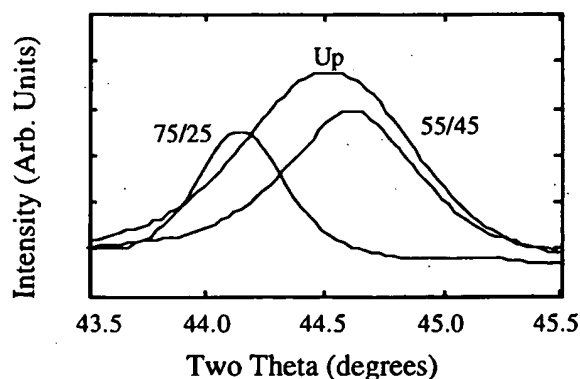


FIG. 3. X-ray diffraction showing (200) peaks of PZT (55/45), PZT (75/25), and "up" films. Peak of "up" film is broad and centralized indicating that a range of compositions between PZT (55/45) and PZT (75/25) is present.

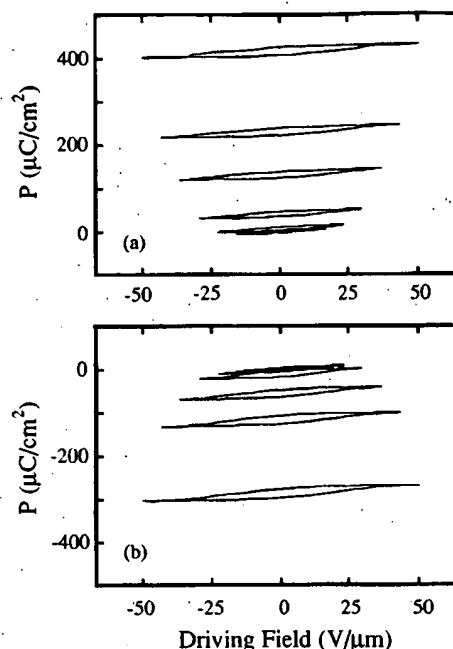


FIG. 4. Polarization offsets of the (a) "up-graded" and the (b) "down-graded" films.

positions of the x-ray peaks for PZT shift with composition.⁸ This is evidenced by the two distinct peaks from 55/45 at $2\theta = 44.65^\circ$ and 75/25 at $2\theta = 44.15^\circ$. The peak from the graded film, however, is broad and centered at $2\theta = 44.45^\circ$, which is consistent with a film having a range of compositions between PZT (55/45) and PZT (75/25). It should be mentioned that the films were highly (111) oriented but interference from the (111) Pt (substrate) peak precluded using the (111) PZT peak for the analysis above.

The results of the hysteresis loop measurements are shown in Fig. 4(a) for the up-graded film and in Fig. 4(b) for the down-graded film. Upon application of a nonzero driving field, the hysteresis loops measured for the graded films immediately began to translate along the polarization axis reaching some equilibrium offset after a few seconds. The loops for the up-graded film translated along the positive polarization axis while those for the down-graded film translated along the negative polarization axis. These translations, or polarization offsets, increased monotonically with driving field E_{max} as shown in Fig. 5 for a typical up-graded film.

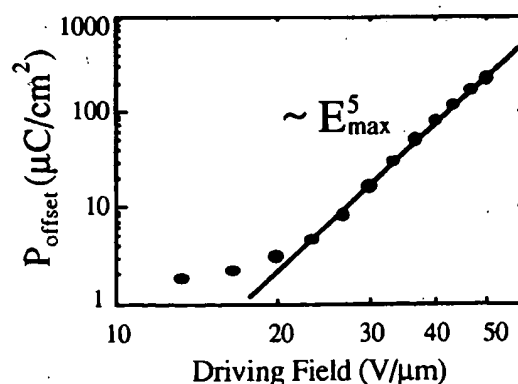


FIG. 5. P_{offset} vs driving field E_{max} . Note the power-law dependence when the driving field exceeds the coercive field.

The offsets increased gradually at low fields. When the driving field was increased beyond $25 \text{ V}/\mu\text{m}$, near the typical coercive field for PZT films, the offsets greatly increased, displaying a power-law dependence on the field given by $P_{\text{offset}} \sim E_{\text{max}}^5$. The largest observed offset, more than $425 \mu\text{C}/\text{cm}^2$ is nearly an order of magnitude greater than any observed in other graded devices.^{1,2}

While asymmetric hysteresis behavior has been observed in conventional films, it has been associated with low resistance and asymmetrical I - V characteristics.⁹ By contrast, the graded films discussed here displayed extremely low dc leakage currents, nearly 100 pA with $\pm 10 \text{ V}$ applied ($10 \text{ G}\Omega$ resistance). In addition, their I - V characteristics were symmetric, which indicates that the polarization offsets are a dynamic rather than static phenomenon. The offset is developed only when an alternating voltage is applied while a dc voltage results only in nominal leakage current.

It was shown that compositionally graded PZT films exhibited large polarization offsets when driven by an alternating electric field. The offsets were nearly an order of magnitude greater than those observed in graded BST devices. This difference is likely due to two factors. First, the spontaneous polarization observed in PZT films ($\sim 30 \mu\text{C}/\text{cm}^2$) is an order of magnitude greater than that typically observed in BST films. Second, the method employed to fabricate the PZT devices resulted in highly oriented, smoothly graded films. Furthermore, the polarization offsets displayed a strong power-law dependence on the applied field when driven with fields above the coercive field. The evidence suggests, then, that the mechanism responsible for the polarization offset requires a smooth composition gradient and is a function of

the spontaneous polarization of the ferroelectric material. This is consistent with one proposed model for graded ferroelectric devices.¹⁰ A broader understanding of graded ferroelectric materials is needed, however, in order to fully exploit their properties in novel device applications. To this end, future experiments are planned to investigate the dependence of the polarization offsets on driving frequency and temperature.

The authors would like to thank D. B. Dimos of Sandia National Laboratories for supplying substrates and J. V. Mantese of General Motors Research and Development Laboratories for many useful discussions. This work was supported in part by the Midwest Superconductivity Consortium (MISCON) DOE Grant No. DE-FG02-90ER45427.

- ¹N. W. Schubring, J. V. Mantese, A. L. Micheli, A. B. Catalan, and R. J. Lopez, *Phys. Rev. Lett.* **68**, 1778 (1992).
- ²J. V. Mantese, N. W. Schubring, A. L. Micheli, A. B. Catalan, M. S. Mohammed, R. Naik, and G. A. Auner, *Appl. Phys. Lett.* **71**, 2047 (1997).
- ³D. Roy and S. B. Krupanidhi, *Appl. Phys. Lett.* **62**, 1056 (1993).
- ⁴B. Jaffe, W. R. Cook, and H. Jaffe, *Piezoelectric Ceramics* (Academic, New York, 1971), pp. 77 and 147.
- ⁵R. Ramesh, K. Luther, B. Wilkens, D. L. Hart, E. Wang, J. M. Tarascon, A. Inam, X. D. Wu, and T. Venkatesan, *Appl. Phys. Lett.* **57**, 1505 (1990).
- ⁶D. Roy, S. B. Krupanidhi, and J. P. Dougherty, *J. Appl. Phys.* **69**, 7930 (1991).
- ⁷C. B. Sawyer and C. H. Tower, *Phys. Rev.* **35**, 269 (1930).
- ⁸F. Jona and G. Shirane, *Ferroelectric Crystals* (Macmillan, New York, 1962), pp. 240-242.
- ⁹K. Abe, S. Komatsu, N. Yanase, K. Sano, and T. Kawakubo, *Jpn. J. Appl. Phys., Part 1* **36**, 5846 (1997).
- ¹⁰J. V. Mantese, N. W. Schubring, A. L. Micheli, and A. B. Catalan, *Appl. Phys. Lett.* **67**, 721 (1995).